BEAMLINE OPTIMIZATION FOR LASER-ACCELERATED IONS

D. Dewitt*, O. Boine-Frankenheim, Technical University of Darmstadt, Darmstadt, Germany

Abstract

Laser-plasma acceleration produces ultrashort, high-brightness ion beams reaching tens of MeV, yet their large divergence and broad energy spread require dedicated capture elements for beam transport. Using laser-accelerated protons from the GSI PHELIX laser to the LIGHT beamline as a reference, we developed a framework to optimize and assess such combined capture and transport systems, with emphasis on injection into conventional accelerators. In addition to our numerical analysis we derive scaling laws linking transmission and chromatic emittance growth to the initial half-opening angle, showing that the present performance is primarily divergence-limited. We also estimate and predict the longitudinal bunch quality and quantify the divergence reduction needed to approach injector-relevant intensities.

INTRODUCTION

Target normal sheath acceleration (TNSA) can produce ion beams with more than 10^{12} particles per shot and very low intrinsic source emittance [1], making it attractive for applications such as conventional accelerator injection [2] and medical applications [3]. Its practical use is nevertheless limited by the large initial divergence and broad energy spread, which make efficient capture and transport challenging. Within the LIGHT project at GSI [2], we numerically optimize a reference beamline consisting of a capture solenoid, a debunching cavity, and a second solenoid to determine the maximum delivered ion number per shot compatible with transverse and longitudinal acceptance constraints. Despite the low intrinsic source emittance, we find that the large divergence and broad energy spread drive strong emittance growth in both the transverse and longitudinal planes.

OPTIMIZATION OF THE LIGHT SETUP FOR MAXIMUM TRANSMISSION

The optimization was performed using a genetic algorithm (GA) [4] coupled to ASTRA [5] through the Python wrapper `lume-astra` [6], followed by a Nelder–Mead refinement step [7]. Space-charge effects were neglected in the present results and are discussed in more detail in [8]. The source was described by a simplified TNSA model with an exponential energy spectrum and an energy-dependent half-opening angle.

Figure 1 shows the transverse envelope and transmission (top) as well as the transverse emittance (bottom) of an optimized beamline for a reference energy of 11.4 MeV.

The transverse emittance initially follows the intrinsic drift growth and then rises sharply at the solenoid entrance. This

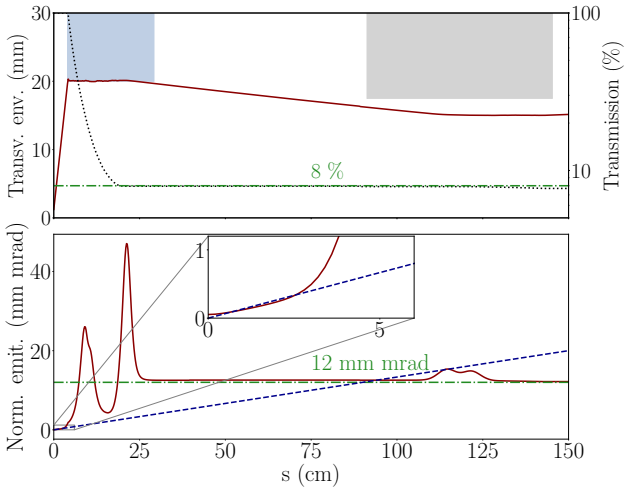

Figure 1: **Top:** Transverse envelope **(red, solid)** and transmission **(black, dotted)** for an optimized beamline. Solenoid and cavity apertures are indicated in blue and gray; the analytical transmission estimate is shown in **(green, dash-dotted)**. **Bottom:** Transverse emittance **(red, solid)** compared with the intrinsic drift growth **(blue, dashed)** and the analytical estimate **(green, dash-dotted)**. All values are 2σ-equivalent.

transient spike is an evaluation artifact of ASTRA's time-based tracking for beams with large energy and temporal spread [9]; after the solenoid, the emittance is dominated by chromatic growth [10]:

$$\varepsilon_\mathrm{n} = \gamma_0\beta_0\alpha f\frac{\Delta E}{E_\mathrm{k}}\theta^2\,. \tag{1}$$

Both emittance and transmission are largely dictated by the first capture solenoid acting on the highly divergent TNSA beam. While the emittance is virtually zero at the source, it increases strongly after the capture element, which can be attributed to the beam divergence and energy spread combined with the chromatic aberrations of the magnetic lens.

Figure 2 shows the longitudinal beam evolution. Before the debunching cavity, the energy spread remains nearly constant and the bunch length increases linearly. The longitudinal emittance growth is approximated by

$$\varepsilon_z = \left(\frac{1}{\beta_0^2\gamma_0^2}\frac{\Delta E}{E_0}\right)d_1E_\mathrm{k}\theta^2\frac{d_0}{d_1} = \frac{\Delta E}{\gamma_0(\gamma_0+1)}d_0\theta^2 \tag{2}$$

and remains nearly constant after capture, apart from local evaluation artifacts near the cavity.

The beam parameters at the end of the LIGHT beamline can be compared with the acceptances of the transfer channel (TK) and SIS18 to estimate the number of particles viable for injection. For typical LIGHT TNSA parameters, the interval 11.4 MeV ± 5% contains about 10^{10} protons at the

* daniel.dewitt@tu-darmstadt.de

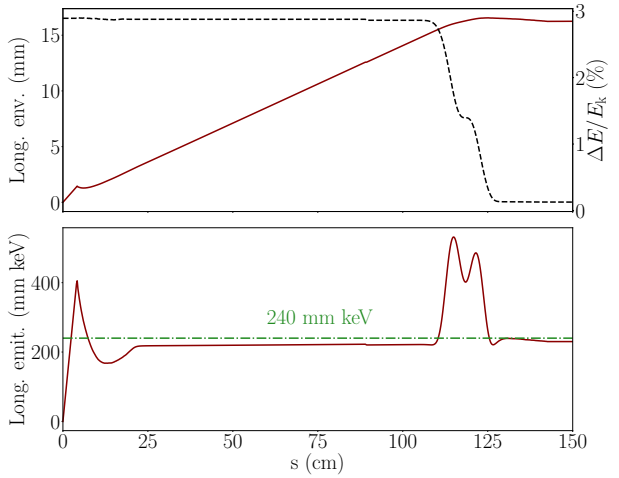

Figure 2: **Top:** Evolution of the longitudinal envelope **(red, solid)** and energy spread **(black, dotted)** relative to the reference energy of 11.4 MeV over s. **Bottom:** Longitudinal emittance along the beamline. The analytical result from Eq. 2 is included as comparison.

Table 1: Reference values and results for injection (inj.) using a solenoid as the capture element. Owing to axial symmetry, the emittances apply to both transverse planes. Highlighted entries indicate the number of protons reaching the TK and SIS18.

Variable	Description	Value	Unit
TK/SIS18 acceptance			
$\mathbf{E_k}$	Reference energy	11.4	MeV
$\mathbf{\Delta E/E_k}$	Energy spread (SIS18)	±0.2	%
$\varepsilon_\mathbf{n}$	Equivalent maximum norm. emittance (TK)	3	mm mrad
Generated beam parameters at TNSA target			
$\theta_\mathbf{max}$	Max. half opening angle	26.5	deg
$\mathbf{\Delta E_S/E_k}$	Initial energy spread	±5	%
$\mathbf{N_{abs}}$	Initial particles	10^{10}	
Simulation results - solenoid			
$\mathbf{N_{TK}}$	**Particles at TK inj.**	8×10^8	
$\varepsilon_{\mathbf{n,TK}}$	Emittance at TK inj.	12	mm mrad
$\mathbf{z_{m,TK}}$	Long. bunch length	15	mm
$\mathbf{\Delta E_{TK}/E_k}$	Energy spread at TK inj.	±0.1	%
$\mathbf{N_{SIS}}$	**Particles exiting TK**	2×10^8	
$\varepsilon_{\mathbf{n,SIS}}$	Emittance at TK exit	3	mm mrad
$\mathbf{\Delta E_{SIS}/E_k}$	Energy spread at TK exit	±0.05	%

source. The optimized beamline delivers 8×10^8 protons to the TK at an emittance of 12 mm mrad and an energy spread of approximately ±0.1%, while the proton yield compatible with SIS18 injection is estimated as 2×10^8. Relative to conventional injectors such as UNILAC [11], laser-accelerated sources can thus approach comparable per-pulse intensities, albeit at substantially lower repetition rates.

SCALING TOWARDS HIGHER INTENSITIES

To identify the most effective parameters for increasing the delivered charge per pulse, we consider the role of the

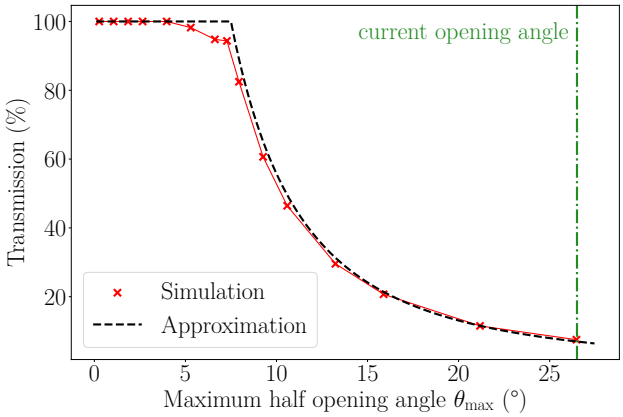

Figure 3: Transmission **(red, solid)** as a function of the initial half-opening angle θ_{max}. The analytical approximation from Eq. 3 **(black, dashed)** is shown for comparison; the typical TNSA value is indicated in **(green, dash-dotted)**.

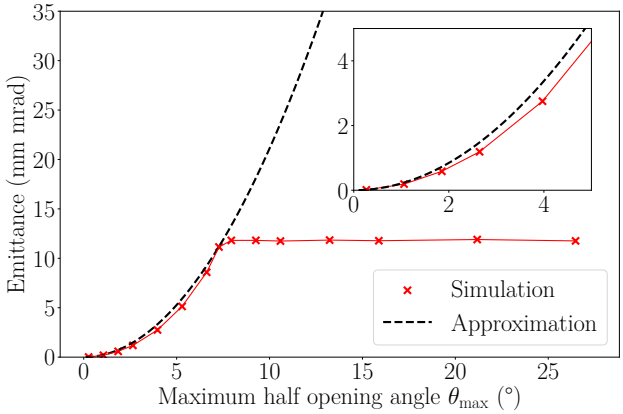

Figure 4: Final normalized emittance **(red, solid)** as a function of the initial half-opening angle. The analytical estimate from Eq. 1 **(black, dashed)** neglects aperture losses.

initial TNSA divergence. Since the TNSA yield scales only weakly with laser intensity, $dN/dE \propto I^{1/3}$ [12–15], reducing the source divergence [16–19] is a more promising route. For a beam with half-opening angle $\theta_0 = \theta_m(E_k)$, the transmission within an energy window ΔE around the reference energy E_k is approximated by

$$\mathcal{T}_0 \approx \left(\frac{\theta_a}{\theta_0}\right)^2 . \tag{3}$$

Figure 3 shows that the optimized simulations follow the expected scaling well. For half-opening angles below 5°, the beam is transmitted through the full beamline without losses, corresponding to a divergence reduction of about 80% relative to present TNSA parameters. In this regime, more than 10^{10} protons pass the capture element.

Figure 4 shows the dependence of the normalized emittance on θ_{max}. For $\theta_{max} < \theta_a$, the emittance follows Eq. 1 and the transmission reaches 100 %. For larger angles, the emittance becomes limited by the beamline acceptance. Thus, increasing the aperture of beamline elements can initially

improve transmission, but only at the cost of accepting a larger emittance and shifting losses further downstream.

The close-up in Fig. 4 highlights the scaling for $\theta_{\max} < 5°$, where the normalized emittance drops below 5 mm mrad. At $\theta_{\max} \approx 4°$, the emittance falls below the TK acceptance, such that the full beam within ΔE is expected to reach the SIS18 injection point. For $\theta_{\max} < 3°$, the emittance drops below 1 mm mrad, making the laser-accelerated beam (within ΔE) comparable to conventional injectors.

CONCLUSION

The present TNSA source-beamline configuration can approach injector-relevant bunch intensities, albeit at repetition rates below those of conventional injectors. Increasing the delivered number of ions per pulse therefore remains a key route to higher average yield. Our analysis indicates that further improvements on the beamline side are limited, with capture-element replacement providing only marginal gains in overall transmission. The analytical scaling laws presented here are consistent with the simulations and enable quantitative target requirements to be formulated for laser-plasma-accelerated protons. In particular, achieving half-opening angles below 5° (a divergence reduction of more than 80 %) appears necessary to reach full transmission through the beamline and to approach injector-relevant operation.

ACKNOWLEDGMENTS

The authors gratefully acknowledge the support of the LIGHT collaboration at GSI Helmholtzzentrum für Schwerionenforschung.

This work is supported by the Deutsche Forschungsgemeinschaft (DFG, German Research Foundation) – Project-ID 499256822 – GRK 2891 'Nuclear Photonics'.

REFERENCES

[1] T. E. Cowan *et al.*, "Ultralow emittance, multi-MeV proton beams from a laser virtual-cathode plasma accelerator", *Phys. Rev. Lett.*, vol. 92, no. 20, p. 204801, May 2004. doi:10.1103/PhysRevLett.92.204801

[2] S. Busold *et al.*, "Shaping laser accelerated ions for future applications – the LIGHT collaboration", *Nuclear Instruments and Methods in Physics Research Section A: Accelerators, Spectrometers, Detectors and Associated Equipment*, vol. 740, pp. 94–98, 2014. doi:10.1016/j.nima.2013.10.025

[3] G. Aymar *et al.*, "LhARA: the laser-hybrid accelerator for radiobiological applications", *Frontiers in Physics*, vol. 8, 2020. doi:10.3389/fphy.2020.567738

[4] A. F. Gad, "Pygad: an intuitive genetic algorithm Python library", *Multimedia Tools and Applications*, vol. 83, pp. 58029–42, 2023. doi:10.48550/arXiv.2106.06158

[5] K. Floettmann, "Astra: a space charge tracking algorithm", 1997, https://www.desy.de/~mpyflo/

[6] C. Mayes, "Python wrapper for Astra", 2020, https://github.com/ChristopherMayes/lume-astra

[7] J. A. Nelder and R. Mead, "A simplex method for function minimization", *The Computer Journal*, vol. 7, no. 4, pp. 308–313, Jan. 1965. doi:10.1093/comjnl/7.4.308

[8] D. C. E. Dewitt, O. Boine-Frankenheim, and A. Blazevic, "Beam intensity and quality predictions for laser-accelerated ions after capture and transport", 2026. https://arxiv.org/abs/2605.09574

[9] K. Floettmann, "Some basic features of the beam emittance", *Phys. Rev. ST Accel. Beams*, vol. 6, no. 3, p. 034202, Mar. 2003. doi:10.1103/PhysRevSTAB.6.034202

[10] I. Hofmann, J. Meyer-ter-Vehn, X. Yan, A. Orzhekhovskaya, and S. Yaramyshev, "Collection and focusing of laser accelerated ion beams for therapy applications", *Phys. Rev. ST Accel. Beams*, vol. 14, no. 3, p. 031304, Mar. 2011. doi:10.1103/PhysRevSTAB.14.031304

[11] W. Barth *et al.*, "Heavy ion linac as a high current proton beam injector", *Phys. Rev. ST Accel. Beams*, vol. 18, no. 5, p. 050102, May 2015. doi:10.1103/PhysRevSTAB.18.050102

[12] P. Mora, "Plasma expansion into a vacuum", *Phys. Rev. Lett.*, vol. 90, no. 18, p. 185002, May 2003. doi:10.1103/PhysRevLett.90.185002

[13] M. G. Haines, M. S. Wei, F. N. Beg, and R. B. Stephens, "Hot-electron temperature and laser-light absorption in fast ignition", *Phys. Rev. Lett.*, vol. 102, no. 4, p. 045008, Jan. 2009. doi:10.1103/PhysRevLett.102.045008

[14] T. Kluge, T. Cowan, A. Debus, U. Schramm, K. Zeil, and M. Bussmann, "Electron temperature scaling in laser interaction with solids", *Phys. Rev. Lett.*, vol. 107, no. 20, p. 205003, Nov. 2011. doi:10.1103/PhysRevLett.107.205003

[15] J. Fuchs *et al.*, "Laser-driven proton scaling laws and new paths towards energy increase", *Nature Physics*, vol. 2, no. 1, pp. 48–54, Jan. 2006. doi:10.1038/nphys199

[16] J. Kim, R. Rajawat, T. Wang, and G. Shvets, "Acceleration and focusing of multispecies ion beam using a converging laser-driven shock", *Phys. Rev. E*, vol. 111, no. 2, p. 025203, Feb. 2025. doi:10.1103/PhysRevE.111.025203

[17] J. Park *et al.*, "Target normal sheath acceleration with a large laser focal diameter", *Physics of Plasmas*, vol. 27, no. 12, p. 123104, Dec. 2020. doi:10.1063/5.0020609

[18] S. Steinke *et al.*, "Acceleration of high charge ion beams with achromatic divergence by petawatt laser pulses", *Phys. Rev. Accel. Beams*, vol. 23, no. 2, p. 021302, Feb. 2020. doi:10.1103/PhysRevAccelBeams.23.021302

[19] T. S. Bauer, "Development, characterization, alignment and experimental validation of partial sphere target arrays for advanced proton acceleration studies", Ph.D. thesis, 2025. doi:10.26083/tuprints-00030072